JOC Article

Effect of Lewis Acid Catalysts on Diels−Alder and Hetero-Diels−Alder Cycloadditions Sharing a Common Transition State

Nihan Çelebi-Ölçüm,[†,‡] Daniel H. Ess,[‡] Viktorya Aviyente,[†] and K. N. Houk*[,‡]

Department of Chemistry and Biochemistry, University of California, Los Angeles, California 90095, and Department of Chemistry, Boğaziçi University, Bebek, Istanbul, 34342, Turkey

houk@chem.ucla.edu

Received May 21, 2008

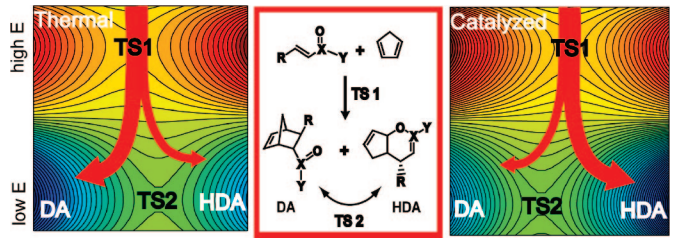

The thermal and Lewis acid catalyzed cycloadditions of β,γ-unsaturated α-ketophosphonates and nitroalkenes with cyclopentadiene have been explored by using density functional theory (DFT) methods. In both cases, only a single highly asynchronous bis-pericyclic transition state yielding both Diels−Alder and hetero-Diels−Alder cycloadducts could be located. Stepwise pathways were found to be higher in energy. On the potential energy surface, the bis-pericyclic cycloaddition transition state is followed by the Claisen rearrangement transition state. No intermediates were located between these transition states. Claisen rearrangement transition states are also highly asynchronous, but bond lengths are skewed in the opposite direction compared to the bis-pericyclic transition states. The relative positions of the bis-pericyclic and Claisen rearrangement transition states may control periselectivity due to the shape of the potential energy surface and corresponding dynamical influences. Inspection of the thermal potential energy surface (PES) indicates that a majority of downhill paths after the bis-pericyclic transition state lead to the Diels−Alder cycloadducts, whereas a smaller number of downhill paths reach the hetero-Diels−Alder products with no intervening energy barrier. Lewis acid catalysts alter the shape of the surface by shifting the cycloaddition and the Claisen rearrangement transition states in opposite directions. This topographical change qualitatively affects the branching ratio after the bis-pericyclic transition state and ultimately reverses the periselectivity of the cycloaddition giving a preference for hetero-Diels−Alder cycloadducts.

Introduction

Two or more reaction pathways sharing a single transition state have been described in a variety of organic reactions.[1] Ess et al. have recently reviewed several examples for organic reactions having these so-called bifurcating potential energy surfaces (PESs).[2] Briefly, on this type of PES (Figure 1), two distinct reaction coordinates give rise to consecutive transition states with no intervening intermediate, and the mechanism is a composite of two steps, although concerted.[3] After the first transition state (TS1, Figure 1), the valley region changes into a ridge region via a valley-ridge inflection point (VRI),[4] due to the requirement of a negative force constant in the orthogonal direction for the subsequent transition state (TS2, Figure 1). The ridge region divides the PES into two separate reaction

[†] University of California, Los Angeles.
[‡] Boğaziçi University.

(1) (a) Kraka, E. In *Encyclopedia of Computational Chemistry*; Schleyer, P. v. R., Ed.; Wiley: New York, 1998; Vol. 4, p 2445. (b) Carpenter, B. K. In *Reactive Intermediate Chemisty*; Moss, R. A., Platz, M. S., Jones, M., Jr., Eds.; Wiley-Interscience: Hoboken, NJ, 2004; pp 925−960. (c) Wenthold, P. G.; Hrovat, D. A.; Borden, W. T.; Lineberger, W. C. *Science* **1996**, *272*, 1456–1459.

(2) Ess, D. H.; Wheeler, S. E.; Iafe, R. G.; Xu, L.; Çelebi-Ölçüm, N.; Houk, K. N. *Angew. Chem.* In press. This review article provides the most complete list of reactions with bifurcating potential energy surfaces.

(3) Singleton, D. A.; Hang, C.; Szymanski, M. J.; Meyer, M. P.; Leach, A. G.; Kuwata, K. T.; Chen, J. S.; Greer, A.; Foote, C. S.; Houk, K. N. *J. Am. Chem. Soc.* **2003**, *125*, 1319–1328.

10.1021/jo801076t CCC: $40.75
Published on Web 09/10/2008

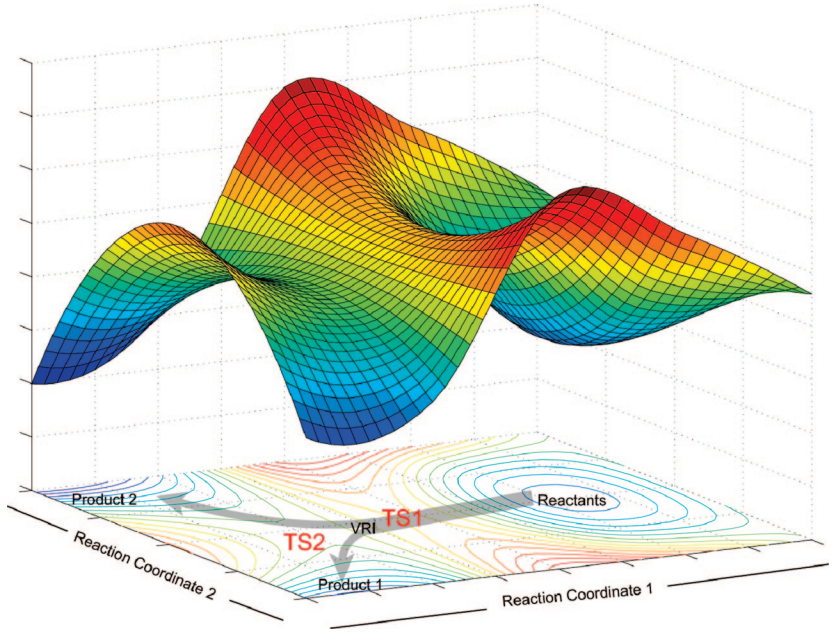

FIGURE 1. Generalized bifurcating potential energy surface. TS1= transition state for reaction coordinate 1. TS2 = transition state for reaction coordinate 2. VRI = valley-ridge inflection point.

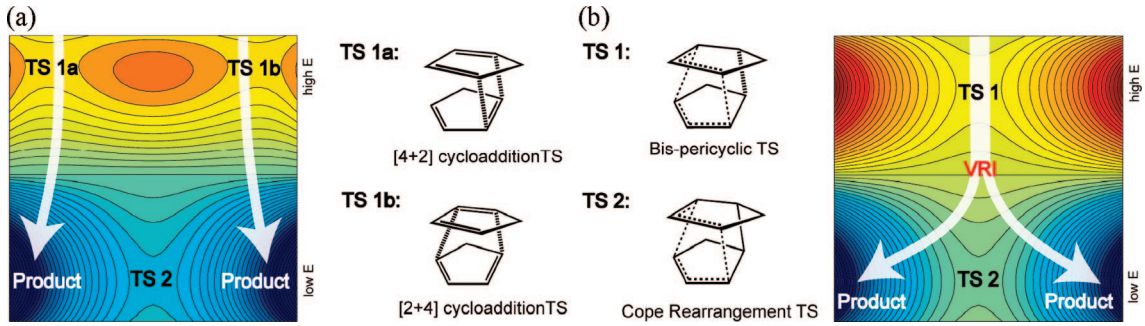

FIGURE 2. (a) Two possible cycloaddition channels for cyclopentadiene dimerization. (b) Caramella's "bis-pericyclic TS" showing merged [4+2] and [2+4] cycloaddition pathways. Periselectivity is controlled by the branching ratio (1:1 in this symmetrical case) in the vicinity of the valley-ridge inflection point (VRI). The two products are identical.

channels. On a symmetrical surface, the common average reaction trajectory branches (bifurcates) from the valley region to follow one of two equivalent reaction pathways near the valley-ridge inflection point, because there is little or no restoring force perpendicular to the first reaction coordinate. It should be noted that the statistical average intrinsic reaction coordinate does not split until the second transition state. However, on such surfaces it is unlikely that any trajectories actually follow the intrinsic reaction coordinate (IRC). In fact, even without a VRI after a transition state, dynamics can allow a reaction path[5] to access multiple products,[6] and the Boltzmann distributions of states at TS1 determine the product distribution ratio.

Generally, when multiple symmetry-allowed processes are possible for a cycloaddition reaction, the periselectivity is classically determined by the difference in activation free energies between the addition channels. Figure 2a shows a hypothetical PES with two distinct reaction pathways for the [4+2] and [2+4] cycloaddition modes of cyclopentadiene dimerization. However, Caramella and co-workers discovered that the actual PES corresponds to a bifurcating surface with a single "bis-pericyclic transition state" where the [4+2] and [2+4] addition modes for cyclopentadiene dimerization have merged (Figure 2b).[7] On this C_s symmetrical hypersurface, the relative abundance of each cycloadduct (periselectivity, although equivalent in this reaction) is controlled by the branching ratio after the bis-pericyclic transition state.[8] After the cycloaddition transition state (TS1, Figure 2b), the downhill IRC leads toward the Cope rearrangement transition state (TS2, Figure 2b) until

(4) (a) Valtazanos, P.; Ruedenberg, K. *Theor. Chim. Acta* **1986**, *69*, 281–307. (b) Xantheas, S.; Elbert, S. T.; Ruedenberg, K. *Theor. Chim. Acta* **1991**, *78*, 365–395. (c) Valtazanos, P.; Ruedenberg, K. *Theor. Chim. Acta* **1991**, *78*, 397–416. (d) Basilevsky, M. V. *Chem. Phys.* **1977**, *24*, 81–89. (e) Quapp, W.; Hirsch, M.; Heidrich, D. *Theor. Chem. Acc.* **1998**, *100*, 285–299. (f) Quapp, W.; Hirsch, M.; Heidrich, D. *Theor. Chem. Acc.* **2000**, *105*, 145–155. (g) Quapp, W. *J. Theor. Comp. Chem.* **2003**, *2*, 385–417. (h) Quapp, W. *J. Mol. Struct.* **2004**, *695–696*, 95–101. (i) Quapp, W.; Hirsch, M.; Heidrich, D. *Theor. Chem. Acc.* **2004**, *112*, 40–51.

(5) See ref 2 for the distinction between reaction pathway, minimum energy pathway, intrinsic reaction coordinate, and valley-ridge inflection, and their relationship to bifurcations. Here we use minimum energy pathway and intrinsic reaction coordinate synonymously.

(6) (a) Sun, L.; Song, K.; Hase, W. L. *Science* **2002**, *296*, 875–878. (b) Mann, D. J. *J. Am. Chem. Soc.* **2002**, *124*, 3208–3209. (c) Lopez, J. G.; Vayner, G.; Lourderaj, U.; Addepalli, S. V.; Kato, S.; de Jong, W. A.; Windrus, T. L.; Hase, W. L. *J. Am. Chem. Soc.* **2007**, *129*, 9976–9985.

(7) Caramella, P.; Quadrelli, P.; Toma, L. *J. Am. Chem. Soc.* **2002**, *124*, 1130–1131.

(8) This does not account for possible rearrangements that may also occur.

SCHEME 1. Possible Diels–Alder and Hetero-Diels–Alder Reactions of Cyclopentadiene with 1a,b

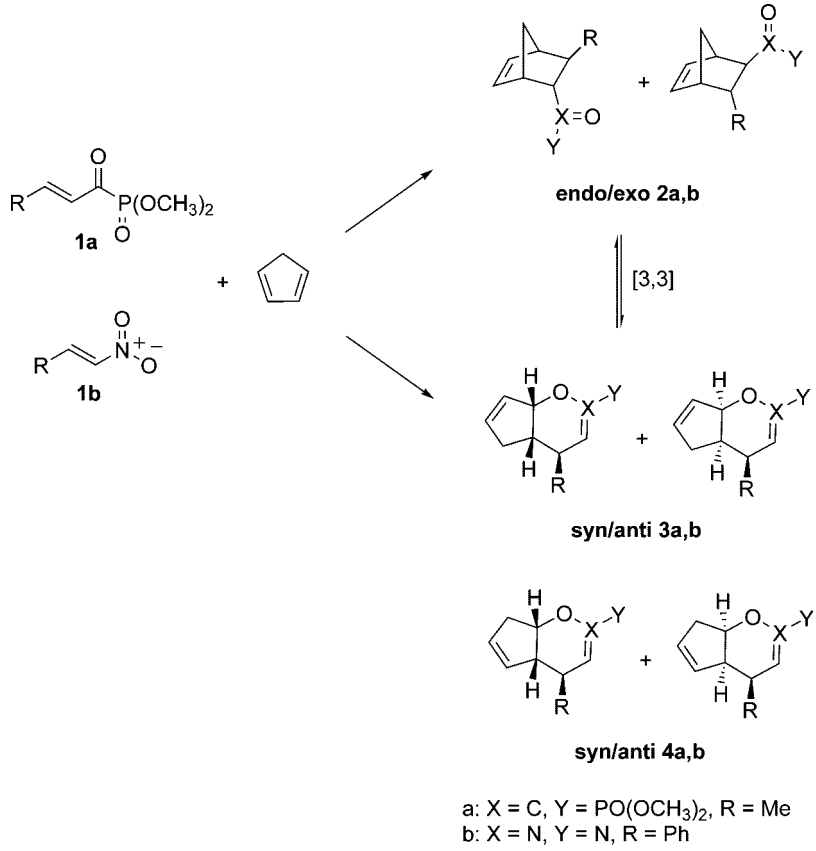

near the VRI. In the vicinity of the VRI, dynamic influences may then dictate the branching ratio from the IRC path. Because the PES of cyclopentadiene dimerization is symmetrical, there will be an exact equal amount of reaction trajectories that take one of two equivalent downhill pathways.

Many of the other previously reported *endo* dimerization reactions that involve bis-pericyclic transition states also lead to equivalent forms of the same product.[9] Bis-pericyclic reactions yielding distinguishable products have unsymmetrical PESs. Houk and co-workers reported cycloaddition bifurcations for the reaction of cycloheptatriene and cyclopentadiene,[10] and for the intramolecular cycloaddition of cyclobutadiene with butadiene.[11] Sastry and co-workers have identified the reaction of cyclopentadiene with phospholes as being akin to bis-pericyclic.[12] Recently, Singleton and co-workers have elegantly shown that the periselectivity ([4+2] versus [2+2]) in the cycloaddition of cyclopentadiene with ketenes is controlled by an unsymmetrical bifurcating PES,[13] rather than the result of two concerted pericyclic processes ([4+2] cycloaddition followed by [3,3] rearrangement).[14]

The highly useful Diels–Alder reactions between dienes and heterodienes often yield two different pericyclic products. Hanessian et al.[15] and Denmark[16] have shown experimentally that the reactions between crotonoyl phosphonates (**1a**) and nitroalkenes (**1b**) with cyclopentadiene (**Cp**) can lead to mixtures of Diels–Alder (**2a**,**b**) and hetero-Diels–Alder (**3a**,**b**) cycloadducts (Scheme 1). In the thermal reactions, cyclopentadiene acts as a 4π component and gives mainly the *endo* and *exo* Diels–Alder cycloadducts, with only minor amounts of the hetero-Diels–Alder cycloadducts (*anti* and *syn*). In the case of *trans*-phenylnitroethylene, the Diels–Alder cycloadduct is formed exclusively. Lewis acids, such as $SnCl_4$, reverse the periselectivity. Cyclopentadiene now acts as the dienophile. The major products formed are the hetero-Diels–Alder cycloadducts with only minor amounts of Diels–Alder products. This change in periselectivity has also been reported by Evans and co-workers for the reaction between cyclopentadiene and **1a** in the presence of Cu-bisoxazoline catalyst.[17]

Besides the classical concerted and stepwise mechanisms leading to each product, a two-step no intermediate mechanism, giving both *endo* Diels–Alder and *anti* hetero-Diels–Alder cycloadducts, is also possible. There is no possibility for a composite *exo* Diels–Alder and *syn* hetero-Diels–Alder transition state. We previously reported the merging of the possible

(9) (a) Toma, L.; Romano, S.; Quadrelli, P.; Caramella, P. *Tetrahedron Lett.* **2001**, *42*, 5077–5080. (b) Quadrelli, P.; Romano, S.; Toma, L.; Caramella, P. *Tetrahedron Lett.* **2002**, *43*, 8785–8789. (c) Quadrelli, P.; Romano, S.; Toma, L.; Caramella, P. *J. Org. Chem.* **2003**, *68*, 6035–6038. (d) Dinadayalane, T. C.; Sastry, G. N. *Organometallics* **2003**, *22*, 5526–5533.

(10) Leach, A. G.; Goldstein, E.; Houk, K. N. *J. Am. Chem. Soc.* **2003**, *125*, 8330–8339.

(11) Limanto, J.; Khuong, K. S.; Houk, K. N.; Snapper, M. L. *J. Am. Chem. Soc.* **2003**, *125*, 16310–16321.

(12) Dinadayalane, T. C.; Gayatri, G.; Sastry, G. N.; Leszczynski, J. *J. Phys. Chem. A* **2005**, *109*, 9310–9323.

(13) Ussing, B. R.; Hang, C.; Singleton, D. A. *J. Am. Chem. Soc.* **2006**, *128*, 7594–7607.

(14) (a) Yamabe, S.; Dai, T.; Minato, T.; Machiguchi, T.; Hasegawa, T. *J. Am. Chem. Soc.* **1996**, *118*, 6518–6519. (b) Yamabe, S.; Minato, T. *J. Org. Chem.* **2000**, *65*, 1830–1841.

(15) Hanessian, S.; Compain, P. *Tetrahedron* **2002**, *58*, 6521–6529.

(16) Denmark, S. E.; Kesler, B. S.; Moon, Y.-C. *J. Org. Chem.* **1992**, *57*, 4912–4924, and references cited therein.

(17) (a) Evans, D. A.; Johnson, J. S. *J. Am. Chem. Soc.* **1998**, *120*, 4895–4896. (b) Evans, D. A.; Johnson, J. S.; Olhava, E. J. *J. Am. Chem. Soc.* **1999**, *122*, 1635–1649.

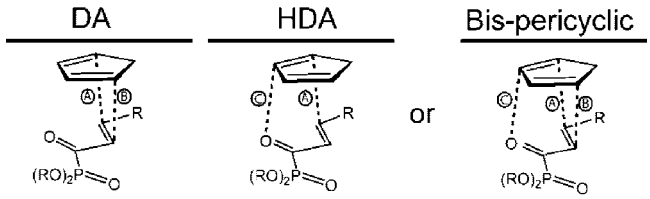

FIGURE 3. Merging of Diels–Alder and Hetero-Diels–Alder transition states for reactions in Scheme 1.

endo Diels–Alder and *anti* hetero-Diels–Alder transition states into a single bis-pericyclic transition state (Figure 3, bonds A, B, and C will be referred to throughout the text).[18] The position of the Claisen rearrangement transition state relative to the bis-pericyclic transition state dictates the PES landscape and branching ratio of the bifurcating reaction pathway. Lewis acid catalyst alters the shape of the PES, shifting the product distribution toward the hetero-Diels–Alder product. We now report details of the possible transition states for concerted and stepwise pathways. We also report the effect of various Lewis acid strengths on the nature of the bis-pericyclic transition state and the shape of the PES.

Computational Methodology. All gas phase geometry optimizations were carried out with Gaussian 03.[19] Stationary points were verified as minima or saddle points by calculation of the full Hessian. Thermodynamic data (see the Supporting Information for enthalpies and free energies) used for zero-point, thermal, and entropy corrections were computed at 298 K. Minimum energy paths were followed by using the intrinsic reaction coordinate as implemented in Gaussian 03.[20] Diradical stationary points were located by using the unrestricted B3LYP formalism. Spin projection energy corrections were done by using the procedure described by Yamaguchi and co-workers.[21] The B3LYP functional was employed with the 6-31+G(d) basis set for crotonoyl phosphonates cycloadditions and the 6-31G(d) for nitroethylene (a model for 1-phenylnitroethylene) cycloadditions. The effective core potential and basis set LANL2DZ was used for all transition metals. Comparative MPW1K/6-31+G(d) distances and energies are given in parentheses. The potential energy surface scans, pictorially presented in the Supporting Information, for the thermal and Lewis acid-catalyzed reactions of cyclopentadiene to **1a** were scanned at 0.05 Å intervals for the formation of bond A and at 0.1 Å intervals for the formation of either bond B or bond C (see Figure 3 definition); in the text this is referred to as the grid of scanned points. Unless noted all values refer to B3LYP geometries and energies and NPA charges.

Results and Discussion

1. Thermal Cycloaddition of Cyclopentadiene to Crotonoyl Phosphonate. One stepwise, seven concerted cycloaddition transition states, and the Claisen rearrangement transition state that interconvert *endo*-Diels–Alder and *anti* hetero-Diels–Alder products were located for the reaction of cyclopentadiene with ***s-cis***- and ***s-trans*-1a** (Figure 4). The lowest energy transition state is the bis-pericyclic transition state **6**[18] ($\Delta H^{\ddagger} = 17.7$ kcal/mol) that can lead to either ***endo*-2a** ($\Delta H = -8.1$ kcal/mol, $\Delta H_{MPW1K} = -25.9$ kcal/mol) or ***anti*-3a** ($\Delta H = -8.2$ kcal/mol, $\Delta H_{MPW1K} = -24.0$ kcal/mol), although the IRC path connects **6** to ***endo*-2a**. Several phosphonate transition state conformations were explored. All others were greater than 1 kcal/mol higher than **6**. No other transition state was found for direct formation of ***anti*-3a**. The alternative route to ***endo*-2a** via transition state **5** is 5.6 kcal/mol higher than **6**. The third "*endo*" transition state, **7**, leads to ***anti*-4a** ($\Delta H = -7.8$ kcal/mol, $\Delta H_{MPW1K} = -23.9$ kcal/mol), but again is significantly higher than **6** (8.4 kcal/mol higher).

The lowest energy *exo* transition state is the addition of cyclopentadiene to ***s-cis*-1a** via transition state **9** ($\Delta H^{\ddagger} = 17.9$ kcal/mol) to give ***exo*-2a** ($\Delta H = -8.5$ kcal/mol, $\Delta H_{MPW1K} = -26.3$ kcal/mol). The transition state, **8**, with ***s-trans*-1a** also gives ***exo*-2a** and is 4.4 kcal/mol higher than **9**. The two other *exo* transition states, **10** and **11**, that give ***syn*-3a** and ***syn*-4a**, respectively ($\Delta H = -9.0$ and -9.1 kcal/mol, $\Delta H_{MPW1K} = -24.6$ and -24.7 kcal/mol), are 4.7 and 8.6 kcal/mol higher in energy than **9**. The difference between the lowest *endo* and lowest *exo* transition state is only 0.2 kcal/mol. Experimentally, Hanessian and Compain observed an endo/exo ratio of 6/1 in neat cyclopentadiene at room temperature during an 8 h reaction time period. They also reported a 7 to 1 ratio of ***endo*-2a** to ***anti*-3a**, which obviously cannot be accounted for by a difference in activation enthalpies, since separate transition states were not located. In accord with the larger activation enthalpies, due to the mismatch of frontier orbital coefficients, neither ***syn*-4a** nor ***anti*-4a** was observed.

A diradical transition state, **12** ($\langle S^2 \rangle = 0.27$), 8.9 kcal/mol higher in energy than **6**, was also located. The energy difference after spin projection is 6.5 kcal/mol. The resulting diradical intermediate is 4.4 kcal/mol higher in energy than **6** (7.3 kcal/mol before spin correction). No other stepwise pathways could be located.

Transition state **6** resembles an asynchronous Diels–Alder transition state with one short partial C–C bond ($r_A = 1.98$ Å) and two longer partial C–C and C–O bonds ($r_B = 2.82$ Å and $r_C = 3.01$ Å). Additional stabilizing secondary orbital overlaps are common to *endo* transition states and set up a rationale for the *endo* selectivity of a variety of Diels–Alder reactions. Generally, the shorter bonds are expected to lead to the major product via the minimum energy pathway while other possible secondary orbital interactions (SOI)[22] are considered to provide additional stabilization to the transition state. However, stabilization of the *endo* transition states via SOIs presumably plays a minor role in this case and competes with the stereoelectronic factors, since no *endo*/*exo* selectivity is predicted. Bond C is about 3 Å and probably this interaction is insufficient to provide substantial stabilization to **6**, which is highly asynchronous and has zwitterionic character (charge separation of 0.3e).

This well-known SOI depicted in bond C, on the other hand, with a distance competitive to bond B, may lead to a more interesting consequence: the merging of the Diels–Alder and hetero-Diels–Alder pathways into **6**. Accordingly, the displacement vectors associated with the imaginary frequency indicate

(18) Çelebi-Ölçüm, N.; Ess, D. H.; Aviyente, V.; Houk, K. N. *J. Am. Chem. Soc.* **2007**, *129*, 4528–4529.
(19) Frisch, M. J.; et al. *Gaussian 03*, Revision D.01; Gaussian, Inc.: Wallingford, CT, 2004.
(20) (a) Gonzalez, C.; Schlegel, H. B. *J. Chem. Phys.* **1989**, *90*, 2154–2161. (b) Gonzalez, C.; Schlegel, H. B. *J. Phys. Chem.* **1990**, *94*, 5523–5527.
(21) (a) Yamaguchi, K.; Jensen, F.; Dorigo, A.; Houk, K. N. *Chem. Phys. Lett.* **1988**, *149*, 537–542. (b) Yamanaka, S.; Kawakami, T.; Nagao, H.; Yamaguchi, K. *Chem. Phys. Lett.* **1994**, *231*, 25–33.
(22) (a) Hoffmann, R.; Woodward, R. B. *J. Am. Chem. Soc.* **1965**, *87*, 4388–4389. (b) Woodward, R. B.; Hoffmann, R. *The Conservation of Orbital Symmetry*; Academic Press: New York, 1970. (c) Salem, L. *J. Am. Chem. Soc.* **1968**, *90*, 553–566. (d) Birney, D. M.; Houk, K. N. *J. Am. Chem. Soc.* **1990**, *112*, 4127–4133.

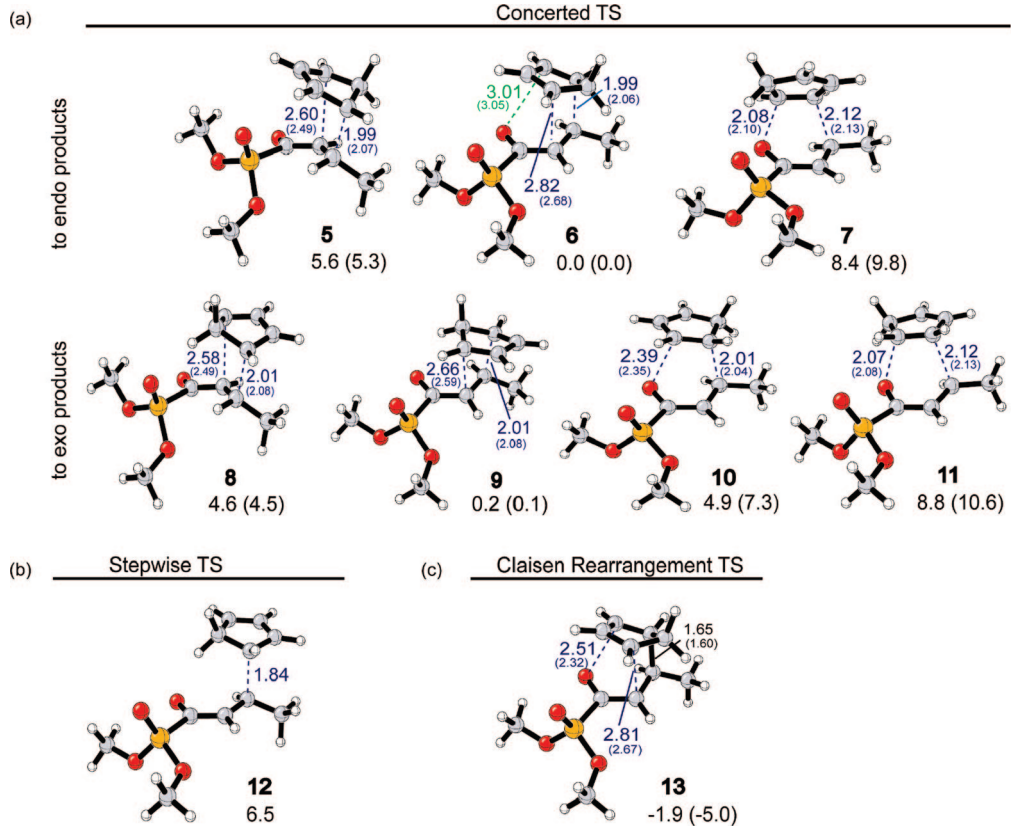

FIGURE 4. Transition state geometries and relative enthalpies (kcal/mol) for the reaction of cyclopentadiene with **1a**. $\Delta H^{\ddagger}_{6} = 17.7$ (13.7) kcal/mol.

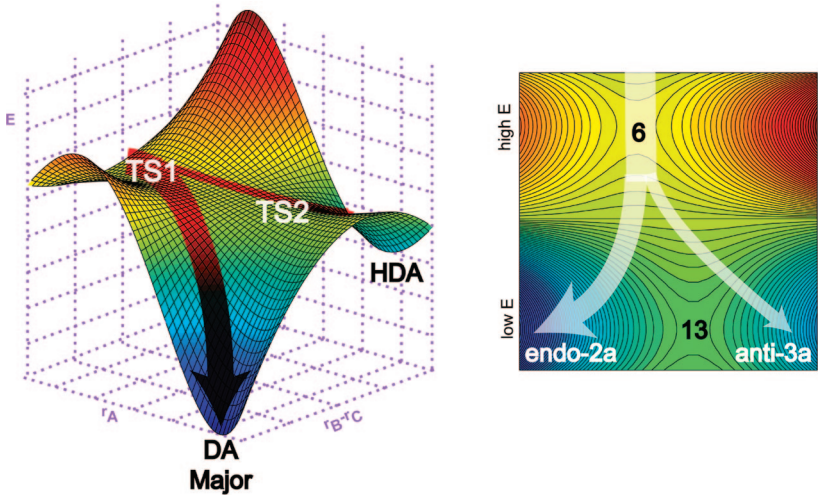

FIGURE 5. Hypothetical potential energy surface of the thermal reaction.

motion along both bonds B and C besides the major vibration along bond A (see the Supporting Information, Figure 3). A detailed exploration of the PES starting from **6** over a grid of approximately 300 points (see the Computational Methodology section for details) shows that the steepest descent leads to ***endo*-2a**, indicative of the bond distance B being smaller than the bond distance C. However, it also shows the presence of alternative downhill paths toward ***anti*-3a**. Although **6** is highly asynchronous and has zwitterionic character, the mechanism is still concerted, since no intermediate exists on the PES and other factors beyond this transition state influence the product distribution.

Figure 4c shows the Claisen rearrangement transition state, **13**[18] (~2 kcal/mol lower than **6**). Compared to the cycloaddition transition state, the Claisen rearrangement transition state has bond lengths skewed in the opposite direction on the PES. Bond length r_C is shorter than r_B ($r_B = 2.81$ Å, $r_C = 2.51$ Å). Figure 5 shows a qualitative PES, based on the grid scan, showing the relative positions of the bis-pericyclic Diels−Alder and Claisen rearrangement transition states (TS1 and TS2). The PES clearly bifurcates in an unsymmetrical fashion (the VRI on this surface is on the path connecting **6** to **13**).[4i] Qualitative inspection of the PES indicates that a larger number of downhill reaction pathways passing through TS1 reach ***endo*-2a** and are probably

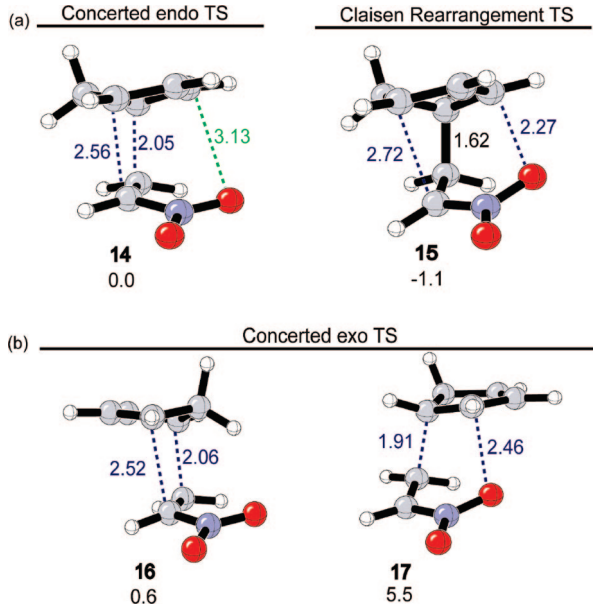

FIGURE 6. Transition state geometries and relative enthalpies for the reaction of cyclopentadiene with **1b**. $\Delta H^{\ddagger}_{14} = 13.3$ kcal/mol.

followed by the majority of reaction trajectories. It is possible that some reaction trajectories passing through TS1 may also follow a smaller number of downhill paths that lead directly to the hetero-Diels–Alder cycloadduct. Ultimately, periselectivity and the product distribution ratio will be mainly determined by the branching ratio from **6**, controlled by the Boltzmann distribution of states at the bis-pericyclic transition state, the exact PES shape, and dynamics on the surface. The amount of hetero-Diels–Alder to Diels–Alder rearrangement may also affect the final product distribution of the cycloaddition. Singleton and co-workers have identified a similar unsymmetrical bifurcating type of PES for the cycloaddition of cyclopentadiene with ketenes and have shown that on such surfaces significant amounts of reaction trajectories can deviate from the statistical average pathway.[13]

2. Thermal Cycloaddition of Cyclopentadiene to Nitroethylene. Figure 6a shows the single *endo* Diels–Alder transition state, **14**,[18] found for the cycloaddition of cyclopentadiene with nitroethylene (a model compound for nitrostyrene, **2b**, $\Delta H^{\ddagger} = 13.3$ kcal/mol). IRC calculations connect **14** to the Diels–Alder adduct, ***endo*-2b** ($\Delta H = -20.6$ kcal/mol). Figure 6a also shows the Claisen rearrangement transition state (**15**[18]) for conversion of the ***endo*-2b** to the hetero-Diels–Alder cycloadduct, **3b** ($\Delta H = -14.4$ kcal/mol). No alternative transition state was located for formation of **3b**. Transition state **14** is highly asynchronous. All three partial bond lengths are different. There is a very advanced C–C bond ($r_A = 2.0$ Å), and the preference for the Diels–Alder adduct occurs because the second C–C bond ($r_B = 2.56$ Å) is 0.57 Å shorter than the C–O interaction ($r_C = 3.13$ Å). The bond lengths in this bis-pericyclic transition state (as well as the much larger $\Delta\Delta H$ between ***endo*-2b** and **3b**) indicate a much stronger preference for Diels–Alder adduct formation compared to the bis-pericyclic transition state with crotonoyl phosphonate.

Again, the Claisen rearrangement transition state, **15**,[18] has partial bond lengths skewed in the opposite direction ($r_B = 2.72$ Å, $r_C = 2.27$ Å) compared to the bis-pericyclic transition state **14**, but are separated by a small change in energy ($\Delta\Delta H = 1.1$ kcal/mol), indicating a flat region of hypersurface. The PES of this reaction is similar to that shown in Figure 5, except it is even more unsymmetrical.

SCHEME 2. Complexes of 1a and $SnCl_4$

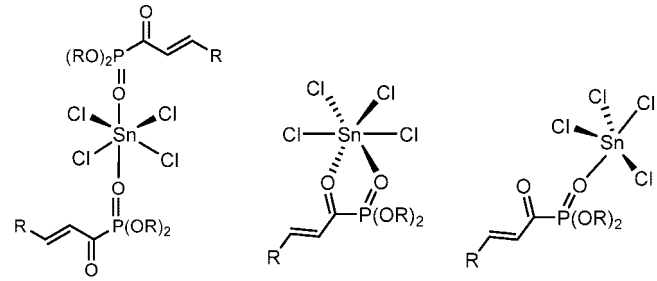

The lowest energy *exo* transition state, **16** ($\Delta H^{\ddagger} = 13.9$ kcal/mol, Figure 6b), gives the ***exo*-2b** ($\Delta H = -20.6$ kcal/mol) product and is predicted to be competitive with **14** ($\Delta\Delta H = 0.6$ kcal/mol). The *exo* transition state, **17**, leading to **3b** is not competitive with a 5.5 kcal/mol higher activation enthalpy. No stepwise transition states or intermediates were located with use of B3LYP and other functionals, presumably because nitro groups are poor radical stabilizers.

3. Lewis Acid-Catalyzed Cycloaddition of Cyclopentadiene with Crotonoyl Phosphonate. There are several possibilities for the coordination of $SnCl_4$ to the dienophile **1a** (Scheme 2). In their experimental work, Telan et al.[23] have studied the coordination of $SnCl_4$ to **1a** using low-temperature (−78 °C) ^{31}P and ^{119}Sn NMR spectroscopy. They reported that, up to 0.5 equiv of $SnCl_4$, a bridged structure (**18**) is formed in which $SnCl_4$ is coordinated with two acylphosphonates via the phosphoryl oxygen to form an octahedral complex. With further addition of $SnCl_4$, **19** is observed in which $SnCl_4$ is coordinated to both phosphoryl and carbonyl oxygens. Complexes **19** and **20** (as a model for **18**) are used in the calculations. In **20**, $SnCl_4$ coordinates to the dienophile via only the phosphoryl oxygen as in **18**, but occupies a trigonal bipyramidal geometry. In both **19** and **20**, Sn is coordinated to the phosphoryl oxygen with a distance of about 2.2 Å (2.22 Å in **19** and 2.15 Å in **20**), whereas in **19**, Sn coordinates also to the carbonyl oxygen but more loosely (2.48 Å). Complex **19** is found to be about 3 kcal/mol destabilized with respect to **20**, presumably due to the loss of flexibility around the C–P bond. The dihedral angle between the carbonyl oxygen and phosphoryl oxygen, which is 96° in **1a**, is 4° in **19** and 114° in **20**.

The destabilization of **19**, however, reverses in the transition state. The distance between Sn and the phosphoryl oxygen does not change much (2.21 Å in **19** and 2.11 Å in **20**), but in **19**, Sn coordinates to the carbonyl oxygen much more tightly (2.24 Å). Accordingly, 0.2e of a total of 0.5e charge transferred (Mulliken) in the transition state is withdrawn by the Lewis acid. On the other hand, no additional charge transfer occurs in the transition states of **20**. The delocalization effect caused by the direct coordination of the Lewis acid to the reaction center in **19** polarizes and eventually stabilizes the transition states. The transition states of **20** lie significantly above the ones obtained from **19** (more than 3.3 kcal/mol), but follow exactly the same trend (see the Supporting Information). In both cases, only a single bis-pericyclic transition state could be located yielding both ***endo*-2a** and ***anti*-3a**.

(23) Telan, L. A.; Poon, C.-D.; Evans, S. A., Jr *J. Org. Chem.* **1996**, *61*, 7455–7462.

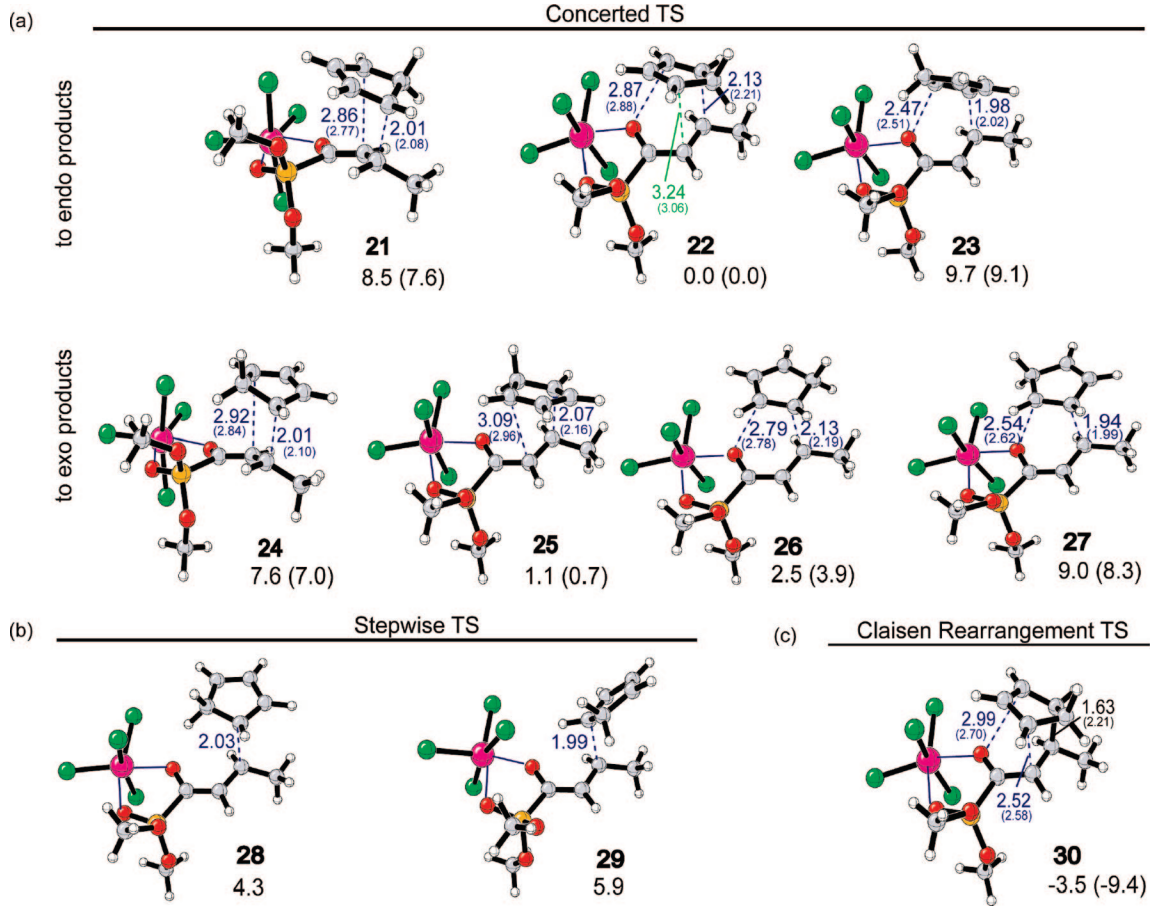

FIGURE 7. Transition state geometries and relative enthalpies for the $SnCl_4$-catalyzed reaction of cyclopentadiene with **1a**. $\Delta H^{\ddagger}_{22} = 9.0$ (3.8) kcal/mol.

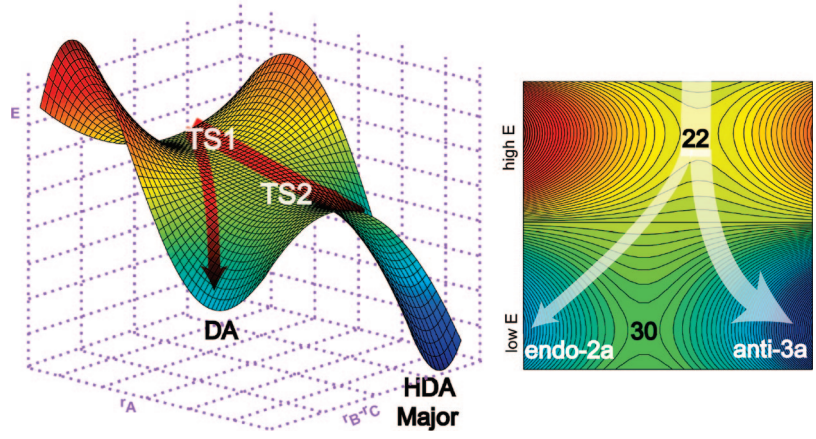

FIGURE 8. Hypothetical potential energy surface of the catalyzed Diels−Alder reaction.

In the products, as in the reactants, the distance between Sn and the phosphoryl oxygen stays around 2.2 Å in all cases. The distance between Sn and the carbonyl oxygen in **19**, however, is 2.49 Å for ***endo*-2a**, and it is as long as 2.66 Å as expected for the hetero-Diels−Alder product, ***anti*-3a**. Complex **19** is discussed here, since 60 mol % of the catalyst was used during the experiments.

Figure 7 shows the transition states and the corresponding relative enthalpies for the potential energy surface of the $SnCl_4$-catalyzed reaction. Similar to the thermal reaction, the lowest energy transition state is the bis-pericyclic transition state **22**[18] ($\Delta H^{\ddagger} = 9.0$ kcal/mol) that may lead to ***anti*-3a** (via the minimum energy pathway) or ***endo*-2a** via an alternative downhill pathway; there is no separate catalyzed transition state directly leading to ***endo*-2a** along a minimum energy pathway. In this bis-pericyclic transition state, bond C is 0.37 Å shorter than bond B, indicative of mostly hetero-Diels−Alder character. Experimentally, Hanessian and Compain found a 1 to 8 ratio of ***endo*-2a** to ***anti*-3a**. The change in the direction of the cycloaddition toward the hetero-Diels−Alder reaction (see **22** compared to **6**) is consistent with the change in the LUMO profiles of ***s-cis*-1a** and its corresponding $SnCl_4$ complex. Coordination of $SnCl_4$ causes a significant decrease in the coefficient of the dienophile α-carbon adjacent to the ketophos-

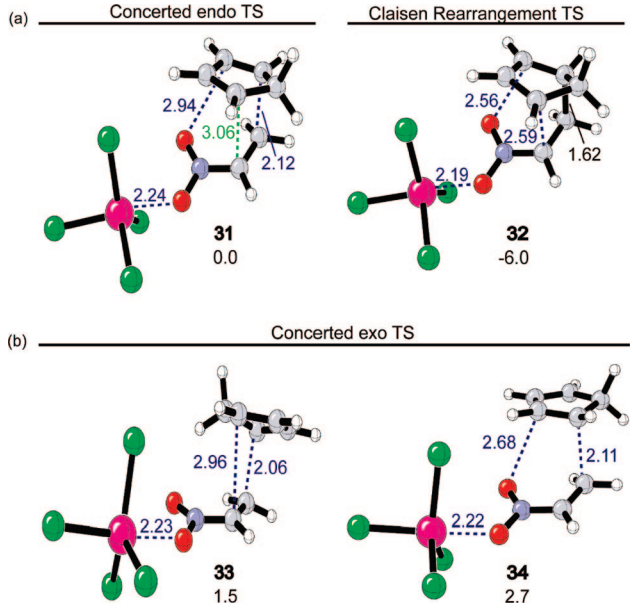

FIGURE 9. Transition state geometries and relative enthalpies for the $SnCl_4$-catalyzed reaction of cyclopentadiene with **1b**. $\Delta H^{\ddagger}_{31} = 5.4$ kcal/mol.

phonate group, and increases the carbonyl–oxygen coefficient (see the Supporting Information). $SnCl_4$ lowers the activation enthalpy of the bis-pericyclic transition state by 8.4 kcal/mol compared to the uncatalyzed reaction.

The alternative reaction pathway giving ***endo*-2a** occurs via transition state **21**, which is significantly higher than **22** (8.5 kcal/mol). Only transition states **25** ($\Delta H^{\ddagger} = 10.1$ kcal/mol) and **26** ($\Delta H^{\ddagger} = 11.5$ kcal/mol) have barriers that are predicted to be reasonably competitive with **22**. These transition states give ***exo*-2a** and ***syn*-3a**. The *endo*/*exo* ratio for this reaction, run in CH_2Cl_2 as the solvent at −78 °C with 0.6 equiv of $SnCl_4$, is 20/1. The computed $\Delta\Delta H$ of 1.1 kcal/mol between **22** and **25** qualitatively agrees with this larger *endo*/*exo* ratio compared to the $\Delta\Delta H$ of only 0.2 kcal/mol between transition states **6** and **9** for the thermal reaction. The degree of diastereocontrol may again be due to steric and electronic factors, since the distance for the SOI displayed in bond B is too long (3.24 Å) to provide extra stabilization to the transition state. Transition states leading to ***anti*-4a** and ***syn*-4a**, **23** and **27**, are 9.7 and 9.0 kcal/mol higher than **22**, and not observed experimentally.

Figure 7b shows the stepwise transition states **28** and **29** that lie 4.3 and 5.9 kcal/mol above **22**, respectively. These transition states are found to be zwitterionic, with $\langle S^2 \rangle$ values of 0. The corresponding intermediates are 0.5 and 0.9 kcal/mol above **22** (see the Supporting Information). In the Claisen rearrangement transition state, **30**[18] (Figure 7c), bond B is shorter ($r_B = 2.52$ Å) than bond C ($r_C = 2.99$ Å). The energy difference between **22** and **30** is more pronounced ($\Delta\Delta H_{B3LYP} = 3.5$ kcal/mol and $\Delta\Delta H_{MPW1K} = 9.4$ kcal/mol) than in the thermal reaction, so the potential energy surface is steeper in this region. A potential energy surface scan on a grid of 400 points shows that only transition state **22** separates reactants and ***anti*-3a** and ***endo*-2a**; the steepest descent from the Lewis acid-catalyzed bis-pericyclic transition state leads to ***anti*-3a**. Although the charge transfer is larger in **22** (0.4e) than in **6**, due to the presence of Lewis acid, the PES shows no intermediates. Figure 8 shows a qualitative representation of the computed Lewis acid-catalyzed PES. Here, the cycloaddition and the Claisen rearrangement transition states are again skewed, but the Lewis acid has shifted the cycloaddition and the Claisen rearrangement transition states in opposite directions (compare to Figure 5). Now most of the reaction trajectories that pass through transition state **22** (also labeled as TS1) may lead to the hetero-Diels–Alder cycloadduct owing to the shape of the PES with surface dynamics allowing reactions to be funneled to the minor Diels–Alder cycloadduct. However, only dynamics simulations would be able to quantitatively give the branching ratio on this PES.

4. Lewis Acid-Catalyzed Cycloaddition of Cyclopentadiene with Nitroethylene. $SnCl_4$ forms an enthalpic complex ($\Delta H = -9$ kcal/mol) with nitroethylene in a monodentate fashion, although the gas phase ΔG of coordination is predicted to be near zero. In the presence of $SnCl_4$, a low-energy bis-pericyclic transition state, **31**,[18] was found. Figure 9a shows **31** and its corresponding Claisen rearrangement transition state, **32**.[18] No Claisen rearrangement transition state could be found for $SnCl_4$ complexation directly to the oxygen involved in bond formation. $SnCl_4$ lowers the barrier by 7.9 kcal/mol ($\Delta H^{\ddagger} = 5.4$ kcal/mol). IRC calculations indicate that **31** leads to the hetero-Diels–Alder adduct, **3b**. No alternative $SnCl_4$-catalyzed transition state was located for ***endo*-2b** formation. **31** has one advanced C–C bond ($r_A = 2.12$ Å), and the preference for C–O bond formation in **31** is shown by a 0.1 Å shorter C–O partial bond length, compared to the longer partial C–C bond ($r_C = 2.94$ Å, $r_B = 3.06$ Å). **32** has nearly equivalent C–O/C–C partial bond lengths ($r_C = 2.56$ Å, $r_B = 2.59$ Å), and the C–C bond length (r_B) is greatly reduced compared to **15**. Under Lewis acid conditions, the reaction of cyclopentadiene with phenylnitroethylene gives exclusively a mixture of ***syn*-3b** and ***anti*-3b** and no ***endo*-2b** or ***exo*-2b**, for which the model nitroethylene dieneophile, **33**, leading to ***exo*-2b**, is 1.5 kcal/mol and **34**, leading to **3b** is 2.7 kcal/mol higher than **31**. ***syn*-4b** and ***anti*-4b** are not formed experimentally.

TABLE 1. Properties of the Bis-pericyclic (TS1) and Claisen Rearrangement (TS2) Transition States (1a + Cyclopentadiene) Catalyzed by Different Lewis Acids

	TS1					TS2			
	charge separation[a]	ΔH^b	*A*	*B*	*C*	ΔH^b	*A*	*B*	*C*
thermal (**6** and **13**)	0.37 (0.30)	17.4	1.99	2.82	3.01	15.4	1.65	2.81	2.51
$SnCl_4$ catalyzed (monodentate complex)	0.43 (0.31)	15.4	2.02	3.01	2.94	12.8	1.64	2.79	2.84
$BiCl_3$ catalyzed	0.46 (0.34)	13.6	2.07	3.16	2.80	10.4	1.64	2.63	2.80
$SnCl_4$ catalyzed (**22** and **30**) (bidentate complex)	0.50 (0.36)	9.0	2.13	3.24	2.87	5.5	1.63	2.52	2.99

[a] Mulliken (NPA) charges. [b] ΔH (kcal/mol) with respect to the reactants.

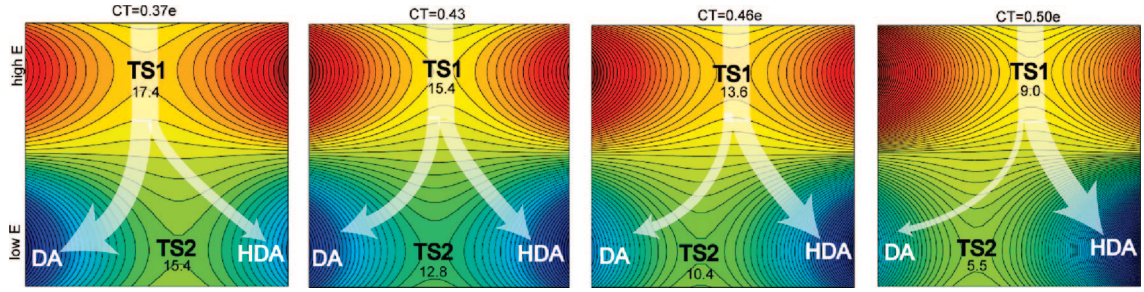

FIGURE 10. Evolution of the potential energy surface with increasing charge transfer (CT) and increasing Lewis acid strength for (left to right) uncatalyzed, $SnCl_4$ monodenate, $BiCl_3$, and $SnCl_4$ bidentate. Transition state enthalpies are given with respect to the reactants (kcal/mol).

Similar to the reaction between cyclopentadiene and **1a**, polarization of the heterodiene LUMO (increase of coefficient at the O atom and decrease at the internal C atom) decreases the C−O bond length and increases the C−C bond length, and now favors bond C over B. Qualitatively this PES is similar to that of crotonoyl phosphonate, except the minimum energy pathway is much steeper decreasing the possibility of reaction dynamics allowing reaction trajectories to lead to the unobserved Diels−Alder cycloadduct after passing through the bis-pericyclic transition state.

5. Effect of Lewis Acid Strength on the PES for Cyclopentadiene Cycloaddition to 1a. To understand the effect of Lewis acids on the shape of bifurcating PESs, we have compared the position of the bis-pericyclic transition state (TS1) and Claisen rearrangement transition state (TS2) using varying strengths of Lewis acidity. Table 1 gives the activation enthalpies, transition state bond lengths (bonds A, B, and C), and charge separation for the uncatalyzed bis-pericyclic and Claisen rearrangement transition states, $SnCl_4$ catalyzed transition states, in which the Lewis acid coordinates to the dienophile either via only the phosphoryl oxygen (monodentate) or via both phosphoryl and carbonyl oxygens (bidentate), and bidentate $BiCl_3$ coordinated transition states. The activation barriers show that the most effective catalyst is the bidentate coordinated $SnCl_4$, lowering the barrier by 8.4 kcal/mol. Monodentate coordination only lowers the activation enthalpy by 2.0 kcal/mol while $BiCl_3$ lowers it by 3.8 kcal/mol. As can be seen from the changes in TS1 bond distance A, catalyzed transition states have longer C−C bond distances corresponding to slightly earlier transition states. With increasing charge separation, the TS1 bond distance B increases gradually from 2.82 Å to 3.24 Å, while bond distance C decreases from 3.01 Å to 2.87 Å. In TS2, however, bond distance B decreases from 2.81 Å to 2.52 Å while bond distance C increases from 2.51 Å to 2.99 Å. Figure 10 shows a qualitative relationship for these four reactions and the position of their bis-pericyclic and Claisen rearrangement transition states. With increasing polar character, the position of TS2 relative to TS1 shifts. In the uncatalyzed reaction TS2 is skewed significantly compared to the position of TS1. However, with monodentate coordination, TS2 becomes skewed in the opposite direction. $BiCl_3$ and bidentate coordination further exacerbates this skewing. Also, as the strength of the Lewis acid increases, the energy difference between TS1 and TS2 increases, indicating a steeper descent along the minimum energy pathway.

Conclusion

The reactions of cyclopentadiene with crotonoyl phosphonates and nitroalkenes proceed through a highly asynchronous bis-pericyclic transition state to give both Diels−Alder and hetero-Diels−Alder cycloadducts. Lewis acids alter the PES landscapes by shifting the relative positions of the cycloaddition and Claisen rearrangement transition states in opposite directions. This change in the shape of the PES ultimately affects the branching ratio and reverses the periselectivity of these bis-pericyclic reactions.

Acknowledgement. We are grateful to the National Science Foundation (U.S.A.), the Scientific and Technological Research Council of Turkey (TUBITAK), the Bogazici University Research Fund (07B501D), and the NIH-FIRCA project (R03TW007177). Computations were performed on the UCLA Academic Technology Services Hoffman Cluster and at the TUBITAK-ULAKBIM High Performance Computing Center. N.Ç.Ö. thanks Onur Temizsoylu for his technical support.

Supporting Information Available: Absolute energies, Cartesian coordinates, PES scans, orbital coefficients, and complete ref 19. This material is available free of charge via the Internet at http://pubs.acs.org.

JO801076T